mathematics

MDPI

Article

Magnetohydrodynamic Motions of Oldroyd-B Fluids in Infinite Circular Cylinder That Applies Longitudinal Shear Stresses to the Fluid or Rotates Around Its Axis

Dumitru Vieru [1,*], Constantin Fetecau [2] and Zulkhibri Ismail [3]

[1] Department of Theoretical Mechanics, Technical University of Iasi, 700050 Iasi, Romania
[2] Academy of Romanian Scientists, 3 Ilfov, 050044 Bucharest, Romania; fetecau@math.tuiasi.ro
[3] Centre for Mathematical Sciences, College of Computing and Applied Sciences, Universiti Malaysia Pahang Al-Sultan Abdullah, Lebuh Persiaran Tun Khalil Yaacob, Kuantan 26300, Pahang, Malaysia; zulkhibri@umpsa.edu.my
* Correspondence: dumitru.vieru@tuiasi.ro or dumitru_vieru@yahoo.com

Abstract: Two classes of magnetohydrodynamic (MHD) motions of the incompressible Oldroyd-B fluids through an infinite cylinder are analytically investigated. General expressions are firstly established for shear stress and velocity fields corresponding to the motion induced by longitudinal shear stress on the boundary. For validation, the expression of the shear stress is determined by two different methods. Using an important remark regarding the governing equations for shear stress and fluid velocity corresponding to the two different motions, this expression is then used to provide the dimensionless velocity field of the MHD motion of the same fluids generated by a cylinder that rotates around its symmetry axis. Obtained results can generate exact solutions for any motion of this kind of Oldroyd-B fluids. Consequently, both types of motions are completely solved. For illustration, some case studies are considered, and adequate velocity fields are provided. The steady-state components of these velocities are presented in different forms whose equivalence is graphically proved. The influence of the magnetic field on the fluid behavior is graphically investigated. It was found that the fluid flows slower, and a steady state is earlier reached in the presence of a magnetic field. The fluid behavior when shear stress is given on the boundary is also investigated.

Keywords: Oldroyd-B fluids; unsteady MHD motions; circular cylinder; general solutions

MSC: 76A05

Citation: Vieru, D.; Fetecau, C.; Ismail, Z. Magnetohydrodynamic Motions of Oldroyd-B Fluids in Infinite Circular Cylinder That Applies Longitudinal Shear Stresses to the Fluid or Rotates Around Its Axis. *Mathematics* **2024**, *12*, 3207. https://doi.org/10.3390/math12203207

Academic Editor: Efstratios Tzirtzilakis

Received: 26 September 2024
Revised: 8 October 2024
Accepted: 9 October 2024
Published: 13 October 2024

1. Introduction

The incompressible Oldroyd-B fluids, which represent an important class of rate-type fluids, have had much success in describing the behavior of many polymeric liquids. They can describe the stress relaxation and the normal stress differences that appear in simple shear flows but do not bring to light shear thinning or shear thickening, which appear in many polymeric materials. In spite of this, the Oldroyd-B model, whose constitutive equations are given by the relations [1]

$$\boldsymbol{T} = -p\boldsymbol{I} + \boldsymbol{S}, \quad \boldsymbol{S} + \lambda \frac{D\boldsymbol{S}}{Dt} = 2\mu \left(\boldsymbol{D} + \lambda_r \frac{D\boldsymbol{D}}{Dt} \right), \tag{1}$$

is amenable to analysis and can describe the behavior of a large class of polymeric liquids. In the above relation, $\boldsymbol{T}$ is the stress tensor, $\boldsymbol{S}$ is the extra-stress tensor, $\boldsymbol{D}$ is the rate of deformation tensor, $-p\boldsymbol{I}$ is the indeterminate stress, p denotes the pressure, μ is the fluid viscosity, λ and λ_r are relaxation and retardation times, and $\frac{D\boldsymbol{S}}{Dt} = \frac{d\boldsymbol{S}}{dt} - \boldsymbol{L}\boldsymbol{S} - \boldsymbol{S}\boldsymbol{L}^T$, $\boldsymbol{L} = grad(\boldsymbol{v})$ is the time upper convected derivative. Here, $\boldsymbol{v}$ is the velocity vector. This model contains incompressible Maxwell and Newtonian fluids when $\lambda = 0$ or $\lambda = \lambda_r = 0$, respectively.

The Oldroyd-B fluids store energy like linearized elastic solids, but their dissipation corresponds to a mixture of two viscous fluids. Some studies have shown that they can model the behavior of many complex fluids like polymer solutions and melts. They can also be used in water filtration systems, oil reservoirs and biomedical fields. This is the reason that exact solutions for different motions of such fluids are important for researchers. They help us to emphasize the fluid behavior in different motion situations or can be used to check numerical schemes that are developed to study more complex motion problems or to establish the accuracy of different approximate solutions. The first exact solutions for unsteady motions of the incompressible Oldroyd-B fluids in cylindrical domains seem to be those of Waters and King [2]. Interesting solutions for other types of motions of same fluids have been established by Rajagopal and Bhatnagar [3], Wood [4], Fetecau [5], Fetecau et al. [6], McGinty et al. [7], Corina Fetecau et al. [8], Jamil and Khan [9], Imran et al. [10] and Ullah et al. [11]. The existence results of weak solutions for steady flows of fluids of Oldroyd type were recently obtained by Baranovskii and Artemov [12].

On the other hand, the MHD motions of fluids have many applications like MHD generators, manufacturing of polymers, plasma studies, biological fluids, nuclear reactors, hydrology and many others. The interplay between a magnetic field and an electrically conducting fluid in motion involves effects with physical and chemical applications. Solutions for MHD motions of electrical conducting incompressible Oldroyd-B fluids (ECIOBFs) in rectangular domains were obtained by Khan et al. [13], Zahid et al. [14] and Ghosh et al. [15]. At the same time, the flow of fluids through porous media has important applications in astrophysics, geophysics, composite manufacturing processes, oil reservoir technology, petroleum industry and agricultural engineering. Exact solutions for MHD motions of ECIOBFs through porous media in rectangular domains were established by Tan and Masuoka [16], Khan et al. [17], Hayat et al. [18], Sultan et al. [19], Khan and Ijaz [20]. There are few exact solutions for such motions of ECIOBFs in cylindrical domains. They were obtained by Hayat et al. [21], Hamza [22], Riaz et al. [23], Fetecau and Vieru [24], and Fetecau et al. [25].

Our interest here is to establish exact general solutions for two classes of unidirectional MHD motions of ECIOBFs in an infinite circular cylinder that rotates around its symmetry axis or applies longitudinal time-dependent shear stresses to the fluid. Firstly, the fluid motion with shear stress on the boundary is investigated, and general expressions are provided for the dimensionless non-trivial shear stress and the fluid velocity. On the basis of a simple observation, one of these expressions is used to give the dimensionless velocity corresponding to motions in which the fluid velocity is prescribed on the boundary. In this way, two important classes of MHD motions of ECIOBFs are completely solved using an infinite circular cylinder. For illustration, some particular cases have been considered, and the corresponding dimensionless velocity fields were used to bring to light some characteristics of the fluid behavior. It was found that the fluid flows slower in the presence of a magnetic field, and the steady state is reached earlier. The correctness of the obtained results is also investigated.

2. Problem Presentation

Consider an electrical conducting incompressible Oldroyd-B fluid (ECIOBF) at rest in an infinite horizontal circular cylinder of radius R. At the moment $t = 0^+$ the cylinder is pulled with time-dependent shear stress $Sf(t)$ along its symmetry axis, and a circular magnetic field of strength B acts perpendicular to this axis. Here, S is a constant shear stress while the function $f(\cdot)$ is piecewise continuous and $f(0) = 0$. Owing to the shear, the fluid is gradually moved, and we are looking for a velocity field of the form

$$\boldsymbol{v} = \boldsymbol{v}(r, t) = (0, 0, u(r, t)), \tag{2}$$

in a suitable system of cylindrical coordinates r, θ and z (Figure 1).

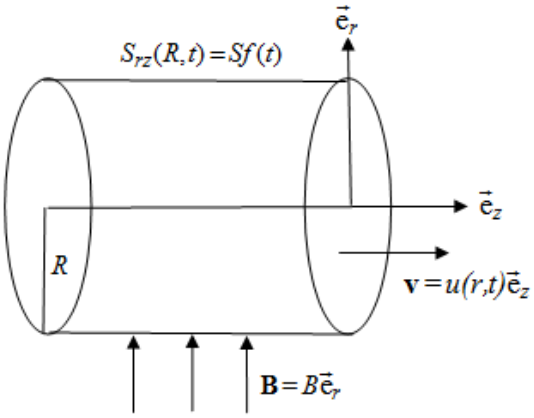

Figure 1. Flow geometry.

Supposing that the extra-stress tensor $\boldsymbol{S}$, as well as the velocity vector $\boldsymbol{v}$, is a function of r and t only and bearing in mind the fact that the fluid has been at rest up to the initial moment $t = 0$, it is easy to show that the non-null shear stress $\eta(r,t) = S_{rz}(r,t)$ must satisfy the next partial differential equation

$$\left(1+\lambda\frac{\partial}{\partial t}\right)\eta(r,t) = \mu\left(1+\lambda_r\frac{\partial}{\partial t}\right)\frac{\partial u(r,t)}{\partial r}\,; \quad 0<r<R, \quad t>0. \tag{3}$$

For such motions, the continuity equation is identically satisfied. We also assume that the fluid is finitely conducting so that the Joule heat due to the presence of an external magnetic field is negligible. In addition, there is no surplus electric charge distribution present in the fluid, the magnetic permeability of the fluid is constant, and the induced magnetic field is negligible in comparison with the applied magnetic field. In these conditions, in the absence of a pressure gradient in the flow direction, the balance of linear momentum reduces to the next relevant partial differential equation [22–24]

$$\rho\frac{\partial u(r,t)}{\partial t} = \frac{\partial \eta(r,t)}{\partial r} + \frac{1}{r}\eta(r,t) - \sigma B^2 u(r,t)\,; \quad 0<r<R, \quad t>0, \tag{4}$$

in which ρ is the fluid density and σ is its electrical conductivity. The corresponding initial and boundary conditions are

$$u(r,0) = \eta(r,0) = 0, \quad 0<r<R; \quad \eta(R,t) = Sf(t), \quad t\geq 0. \tag{5}$$

The dimensionless forms of the governing Equations (3) and (4), namely

$$\left(1+\alpha\frac{\partial}{\partial t}\right)\eta(r,t) = \left(1+\beta\frac{\partial}{\partial t}\right)\frac{\partial u(r,t)}{\partial r}; \quad 0<r<1, \quad t>0, \tag{6}$$

$$\frac{\partial u(r,t)}{\partial t} = \frac{\partial \eta(r,t)}{\partial r} + \frac{1}{r}\eta(r,t) - Mu(r,t); \quad 0<r<1, \quad t>0, \tag{7}$$

have been obtained using the next non-dimensional variables and functions

$$r^* = \frac{1}{R}r, \quad t^* = \frac{\nu}{R^2}t, \quad u^* = \frac{\mu}{RS}u, \quad \eta^* = \frac{1}{S}\eta, \quad f^*(t^*) = f\left(\frac{R^2}{\nu}t^*\right) \tag{8}$$

and renouncing to the star notation.

The corresponding initial and boundary conditions are

$$u(r,0) = \eta(r,0) = 0, \quad 0<r<1; \quad \eta(1,t) = f(t), \quad t\geq 0, \tag{9}$$

while the magnetic parameter M and the constants α, β are defined by the relations

$$M = \frac{\sigma B^2}{\rho}\frac{R^2}{\nu} = \frac{R^2}{\mu}\sigma B^2, \quad \alpha = \frac{\nu\lambda}{R^2}, \quad \beta = \frac{\nu\lambda_r}{R^2}. \tag{10}$$

Exact solutions for MHD motions of a larger class of rate-type fluids through a porous medium were recently obtained by Fetecau et al. [26] when a differential expression of shear stress is prescribed on the boundary.

3. General Solutions

In this section, using the Laplace and finite Hankel transforms, we determine closed-form expressions for the dimensionless shear stress and velocity fields corresponding to the abovementioned MHD motion of ECIOBFs. By applying the Laplace transform to the Equalities (6) and (7) and bearing in mind the corresponding initial conditions, one finds the transformed governing equations

$$(\alpha\, s + 1)\overline{\eta}(r,s) = (\beta\, s + 1)\frac{\partial \overline{u}(r,s)}{\partial r}; \quad 0 < r < 1, \tag{11}$$

$$s\overline{u}(r,s) = \frac{\partial \overline{\eta}(r,s)}{\partial r} + \frac{1}{r}\overline{\eta}(r,s) - M\overline{u}(r,s); \quad 0 < r < 1, \tag{12}$$

in which $\overline{\eta}(r,s)$ and $\overline{u}(r,s)$ are the Laplace transforms of $\eta(r,t)$ and $u(r,t)$, respectively.

3.1. Determination of Shear Stress

Eliminating transformed velocity $\overline{u}(r,s)$ between Equations (11) and (12) and bearing in mind the boundary condition (9), one finds the following boundary value problem

$$\frac{1}{r}\frac{\partial}{\partial r}\left[r\frac{\partial \overline{\eta}(r,s)}{\partial r}\right] - \frac{1}{r^2}\overline{\eta}(r,s) = a(s)\overline{\eta}(r,s); \quad \overline{\eta}(1,s) = \overline{f}(s), \tag{13}$$

for the function $\overline{\eta}(r,s)$. In the above relation, $\overline{f}(s)$ is the Laplace transform of $f(t)$ while

$$a(s) = \frac{(\alpha s + 1)(s + M)}{\beta s + 1}. \tag{14}$$

By multiplying Equation (13) by $rJ_1(rr_n)$, where $J_1(\cdot)$ is the standard Bessel function of the first kind and one order and r_n are the positive roots of the transcendental equation $J_1(r) = 0$, integrating the result between zero and one and bearing in mind the next identity

$$\int_0^1 J_1(rr_n)\frac{\partial}{\partial r}\left[r\frac{\partial \overline{\eta}(r,s)}{\partial r}\right]dr = -r_n^2\overline{\eta}_H(r_n,s) - r_n\overline{\eta}(1,s)J_0(r_n), \tag{15}$$

one obtains for the finite Hankel transform $\overline{\eta}_H(r_n,s)$ of $\overline{\eta}(r,s)$ the next expression

$$\overline{\eta}_H(r_n,s) = -\frac{r_n J_0(r_n)}{r_n^2 + a(s)}\overline{f}(s). \tag{16}$$

In the above relations, the finite Hankel transform $\overline{\eta}_H(r_n,s)$ and its inverse $\overline{\eta}(r,s)$ are defined by the next relations [27]:

$$\overline{\eta}_H(r_n,s) = \int_0^1 r\overline{\eta}(r,s)J_1(rr_n)dr, \quad \overline{\eta}(r,s) = 2\sum_{n=1}^{\infty}\frac{J_1(rr_n)}{J_0^2(r_n)}\overline{\eta}_H(r_n,s). \tag{17}$$

For a suitable form of the final result, we rewrite $\overline{\eta}_H(r_n, s)$ in the equivalent form

$$\overline{\eta}_H(r_n, s) = -\frac{J_0(r_n)}{r_n}\overline{f}(s) + \overline{f}(s)\frac{J_0(r_n)}{r_n}\frac{a(s)}{r_n^2 + a(s)} \tag{18}$$

and apply the inverse finite Hankel transform. This results in the following:

$$\overline{\eta}(r, s) = r\overline{f}(s) + 2\overline{f}(s)\sum_{n=1}^{\infty}\frac{J_1(rr_n)}{r_n J_0(r_n)}\overline{F}_n(s); \quad \overline{F}_n(s) = \frac{a(s)}{r_n^2 + a(s)}. \tag{19}$$

Now, we rewrite $\overline{F}_n(s)$ in the convenient form

$$\overline{F}_n(s) = 1 - \frac{r_n^2}{\alpha}\left[\beta\frac{s + c_n}{(s + c_n)^2 - d_n^2} + \frac{1 - \beta c_n}{d_n}\frac{d_n}{(s + c_n)^2 - d_n^2}\right], \tag{20}$$

where

$$c_n = \frac{\beta r_n^2 + \alpha M + 1}{2\alpha}, \quad d_n = \frac{\sqrt{(\beta r_n^2 + \alpha M + 1)^2 - 4\alpha(r_n^2 + M)}}{2\alpha} \tag{21}$$

and apply the inverse Laplace transform. Using the identities (A1) from Appendix A, one obtains the inverse Laplace transform $F_n(t)$ of $\overline{F}_n(s)$ in the form

$$F_n(t) = \delta(t) - \frac{r_n^2}{\alpha}\left[\beta\cosh(d_n t) + \frac{1 - \beta c_n}{d_n}\sinh(d_n t)\right]\mathrm{e}^{-c_n t}, \tag{22}$$

where $\delta(\cdot)$ is the Dirac delta function.

Finally, applying the inverse Laplace transform to the first equality (19) and bearing in mind Equation (22), one obtains the dimensionless shear stress $\eta(r, t)$ corresponding to the motion in the discussion of ECIOBFs in the form

$$\begin{aligned}&\eta(r, t) = rf(t)\\ &+2\sum_{n=1}^{\infty}\frac{J_1(rr_n)}{r_n J_0(r_n)}\left\{f(t) - \frac{r_n^2}{\alpha}\left[\beta\cosh(d_n t) + \frac{1 - \beta c_n}{d_n}\sinh(d_n t)\right]\mathrm{e}^{-c_n t} * f(t)\right\},\end{aligned} \tag{23}$$

where $*$ denotes the convolution product of the two functions. The shear stress given by the Equality (23) satisfies both the initial and boundary conditions. In Appendix A, for the validation of this last result, the same expression for the dimensionless shear stress $\eta(r, t)$ has been established using the theorem of residues.

3.2. Determination of the Fluid Velocity

From the Equality (12), it immediately results that

$$\overline{u}(r, s) = \frac{1}{s + M}\left(\frac{\partial}{\partial r} + \frac{1}{r}\right)\overline{\eta}(r, s), \tag{24}$$

in which, as it results from the Equations (16) and (17),

$$\overline{\eta}(r, s) = 2\sum_{n=1}^{\infty}\frac{J_1(rr_n)}{J_0^2(r_n)}\overline{\eta}_H(r_n, s) = -2\overline{f}(s)\sum_{n=1}^{\infty}\frac{r_n J_1(rr_n)}{[r_n^2 + a(s)]J_0(r_n)}. \tag{25}$$

Direct computations show that

$$\frac{\partial\overline{\eta}(r, s)}{\partial r} + \frac{1}{r}\overline{\eta}(r, s) = -2\overline{f}(s)\sum_{n=1}^{\infty}\frac{r_n^2 J_0(rr_n)}{[r_n^2 + a(s)]J_0(r_n)}. \tag{26}$$

From the Equalities (24) and (26) it results that

$$\overline{u}(r,s) = -2\overline{f}(s)\sum_{n=1}^{\infty}\frac{r_n^2 J_0(rr_n)}{J_0(r_n)}\overline{G}_n(s);\ \ \overline{G}_n(s) = \frac{1}{(s+\mathrm{M})[r_n^2+a(s)]}. \tag{27}$$

By writing $\overline{G}_n(s)$ in the convenient form, namely

$$\overline{G}_n(s) = \frac{1}{\alpha}\left[\frac{x_n}{s+M} + \frac{y_n}{s-s_{1n}} + \frac{z_n}{s-s_{2n}}\right], \tag{28}$$

where $s_{1n} = -c_n + d_n < 0,\ \ s_{2n} = -c_n - d_n < 0$ and

$$\begin{aligned} x_n &= -\tfrac{\beta M-1}{(s_{1n}+M)(s_{2n}+M)},\ \ y_n = \tfrac{\beta s_{1n}+1}{(s_{1n}-s_{2n})(s_{1n}+M)}, \\ z_n &= -\tfrac{\beta s_{2n}+1}{(s_{1n}-s_{2n})(s_{2n}+M)} \end{aligned} \tag{29}$$

and applying the inverse Laplace transform to Equation (28), one finds that

$$G_n(t) = \frac{1}{\alpha}\left[x_n \mathrm{e}^{-Mt} + y_n \mathrm{e}^{-(c_n-d_n)t} + z_n \mathrm{e}^{-(c_n+d_n)t}\right]. \tag{30}$$

Consequently, applying the inverse Laplace transform to Equation (27) and bearing in mind the Equality (30), one obtains the dimensionless velocity field $u(r,t)$ in the form

$$u(r,t) = -\frac{2}{\alpha}\sum_{n=1}^{\infty}\frac{r_n^2 J_0(rr_n)}{J_0(r_n)} f(t) * \left[x_n \mathrm{e}^{-Mt} + y_n \mathrm{e}^{-(c_n-d_n)t} + z_n \mathrm{e}^{-(c_n+d_n)t}\right], \tag{31}$$

or equivalently

$$\begin{aligned} u(r,t) = &-\frac{2f(t)}{\alpha}\sum_{n=1}^{\infty}\frac{r_n^2 J_0(rr_n)}{J_0(r_n)}\left(\frac{x_n}{M} + \frac{y_n}{c_n-d_n} + \frac{z_n}{c_n+d_n}\right) \\ &+\frac{2}{\alpha}\sum_{n=1}^{\infty}\frac{r_n^2 J_0(rr_n)}{J_0(r_n)} f'(t) * \left[\frac{x_n}{\mathrm{M}}\mathrm{e}^{-Mt} + \frac{y_n}{c_n-d_n}\mathrm{e}^{-(c_n-d_n)t} + \frac{z_n}{c_n+d_n}\mathrm{e}^{-(c_n+d_n)t}\right]. \end{aligned} \tag{32}$$

Finally, it is worth pointing out the fact that similar solutions for the electrical conducting incompressible Maxwell fluids performing the same motion can be immediately obtained, making $\beta = 0$, as in the previous relations.

4. Application

Let us now consider the MHD motion of the same ECIOBFs through a porous medium generated by the infinite circular cylinder at the moment $t = 0^+$ begins to rotate around its symmetry axis with the time-dependent velocity $Vg(t)$. Here, V is a constant velocity, while the piecewise continuous function $g(\cdot)$ has a zero value in $t = 0$. The corresponding velocity vector $\boldsymbol{w}$ is given by the relation

$$\boldsymbol{w} = \boldsymbol{w}(r,t) = (0, w(r,t), 0), \tag{33}$$

in the same system r, θ and z of cylindrical coordinates. Assuming again that the extra-stress tensor $\boldsymbol{S}$ is a function of r and t and the fact that the fluid has been at rest up to the initial moment $t = 0$, it is not difficult to show that the non-trivial shear stress $\tau(r,t) = S_{r\theta}(r,t)$ has to satisfy the next partial differential equation

$$\left(1 + \lambda\frac{\partial}{\partial t}\right)\tau(r,t) = \mu\left(1 + \lambda_r\frac{\partial}{\partial t}\right)\left[\frac{\partial w(r,t)}{\partial r} - \frac{1}{r}w(r,t)\right];\quad 0 < r < R,\quad t > 0. \tag{34}$$

The continuity equation is also satisfied while the balance of momentum, in the same conditions as in Section 2, reduces to the partial differential equation

$$\rho\frac{\partial w(r,t)}{\partial t}=\frac{\partial \tau(r,t)}{\partial r}+\frac{2}{r}\tau(r,t)-\sigma B^2 w(r,t);\quad 0<r<R,\quad t>0. \tag{35}$$

The corresponding initial and boundary conditions are

$$w(r,0)=\ \eta(r,0)=0,\quad 0<r<R;\quad w(r,t)=Vg(t),\quad t\geq 0. \tag{36}$$

By introducing the following non-dimensional variables and functions

$$r^*=\frac{1}{R}r,\quad t^*=\frac{\nu}{R^2}t,\quad w^*=\frac{1}{V}w,\quad \tau^*=\frac{R}{\mu V}\tau,\quad g^*(t^*)=g\left(\frac{R^2}{\nu}t^*\right), \tag{37}$$

and eliminating the star notation, one obtains the dimensionless forms

$$\left(1+\alpha\frac{\partial}{\partial t}\right)\tau(r,t)=\left(1+\beta\frac{\partial}{\partial t}\right)\left[\frac{\partial w(r,t)}{\partial r}-\frac{1}{r}w(r,t)\right];\quad 0<r<1,\quad t>0, \tag{38}$$

$$\frac{\partial w(r,t)}{\partial t}=\frac{\partial \tau(r,t)}{\partial r}+\frac{2}{r}\tau(r,t)-Mw(r,t);\quad 0<r<1,\quad t>0, \tag{39}$$

of the governing equations. The corresponding initial and boundary conditions are

$$w(r,0)=\tau(r,0)=0,\quad 0<r<1;\quad w(1,t)=g(t),\quad t\geq 0. \tag{40}$$

Eliminating $\tau(r,t)$ between Equations (38) and (39), one finds the governing equation

$$\begin{array}{l}\left(1+\alpha\frac{\partial}{\partial t}\right)\frac{\partial w(r,t)}{\partial t}=\left(1+\beta\frac{\partial}{\partial t}\right)\left[\frac{\partial^2}{\partial r^2}+\frac{1}{r}\frac{\partial}{\partial r}-\frac{1}{r^2}\right]w(r,t)\\ -M\left(1+\alpha\frac{\partial}{\partial t}\right)w(r,t);\quad 0<r<1,\quad t>0,\end{array} \tag{41}$$

for the dimensionless velocity field $w(r,t)$ corresponding to the present motion of ECIOBFs. Now, it is worth observing and using the fact that this partial differential equation is identical in form to the governing equation

$$\begin{array}{l}\left(1+\alpha\frac{\partial}{\partial t}\right)\frac{\partial \eta(r,t)}{\partial t}=\left(1+\beta\frac{\partial}{\partial t}\right)\left[\frac{\partial^2}{\partial r^2}+\frac{1}{r}\frac{\partial}{\partial r}-\frac{1}{r^2}\right]\eta(r,t)\\ -M\left(1+\alpha\frac{\partial}{\partial t}\right)\eta(r,t);\quad 0<r<1,\quad t>0,\end{array} \tag{42}$$

of the non-dimensional shear stress $\eta(r,t)$ obtained, eliminating the velocity $u(r,t)$ between the governing Equations (6) and (7) of Section 2.

Since the initial and boundary conditions corresponding to the two different MHD motions of ECIOBFs are also identical in form, it results that the velocity field $w(r,t)$ corresponding to the present motion is given by the relation (see the equality (23))

$$\begin{array}{l}w(r,t)=rg(t)\\ +2\sum\limits_{n=1}^{\infty}\frac{J_1(rr_n)}{r_nJ_0(r_n)}\left\{g(t)-\frac{r_n^2}{\alpha}\left[\beta\cosh(d_nt)+\frac{1-\beta c_n}{d_n}\sinh(d_nt)\right]\mathrm{e}^{-c_nt}*g(t)\right\}.\end{array} \tag{43}$$

As soon as the dimensionless fluid velocity is known, the corresponding shear stress can be determined using the Laplace transform or solving the ordinary linear differential Equation (38) with the corresponding initial condition. Consequently, the MHD motion problem of ECIOBFs in an infinite circular cylinder that rotates around its symmetry axis is completely solved. For illustration, as well as to shed light on some characteristics of the fluid behavior, some study cases are considered.

4.1. The Study Case When Cylinder Oscillates around Its Symmetry Axis

By substituting the function $g(t)$ by $H(t)\cos(\omega t)$ or $H(t)\sin(\omega t)$ in Equation (43), one finds the dimensionless starting velocities $w_c(r,t)$ and $w_s(r,t)$ corresponding to the MHD motion of ECIOBFs induced by the circular cylinder that executes cosine or sine oscillations, respectively, around its symmetry axis. Here, $H(t)$ is the Heaviside unit step function, and ω is the non-dimensional frequency of the oscillations. In the following we show that both motions become steady in time and the dimensionless starting velocity fields $w_c(r,t)$ and $w_s(r,t)$ can be written as sum of their steady state and transient components, namely

$$w_c(r,t) = [w_{cs}(r,t) + w_{ct}(r,t)]H(t), \quad w_s(r,t) = [w_{ss}(r,t) + w_{st}(r,t)]H(t). \tag{44}$$

Therefore, the convolution product from Equation (43) has to be evaluated. Lengthy but straightforward computations show that

$$\begin{aligned} &\tfrac{r_n^2}{\alpha}\left[\beta\cosh(d_n t) + \tfrac{1-\beta c_n}{d_n}\sinh(d_n t)\right] \mathrm{e}^{-c_n t} * H(t)\cos(\omega t) \\ &= x_n\cos(\omega t) + y_n\sin(\omega t) - [x_n\cosh(d_n t) + u_n\sinh(d_n t)]\,\mathrm{e}^{-c_n t}, \end{aligned} \tag{45}$$

$$\begin{aligned} &\tfrac{r_n^2}{\alpha}\left[\beta\cosh(d_n t) + \tfrac{1-\beta c_n}{d_n}\sinh(d_n t)\right]\mathrm{e}^{-c_n t} * H(t)\sin(\omega t) \\ &= -y_n\cos(\omega t) + x_n\sin(\omega t) + [y_n\cosh(d_n t) - v_n\sinh(d_n t)]\,\mathrm{e}^{-c_n t}, \end{aligned} \tag{46}$$

where the constants x_n, y_n, u_n and v_n are given by the relations

$$\begin{aligned} x_n &= r_n^2\,\tfrac{r_n^2+M+\omega^2(\beta^2 r_n^2+\alpha\beta M+\beta-\alpha)}{(r_n^2+M-\alpha\omega^2)^2+(2\alpha\omega c_n)^2}, \\ y_n &= \omega r_n^2\,\tfrac{\alpha\beta\omega^2+(\alpha-\beta)M+1}{(r_n^2+M-\alpha\omega^2)^2+(2\alpha\omega c_n)^2}, \\ u_n &= \tfrac{\alpha}{d_n}\tfrac{r_n^2}{}\,\tfrac{c_n(c_n^2-d_n^2+\omega^2)-\beta(c_n^2-d_n^2)^2-\beta\omega^2(c_n^2+d_n^2)}{(r_n^2+M-\alpha\omega^2)^2+(2\alpha\omega c_n)^2}, \\ v_n &= \tfrac{\alpha\omega}{d_n}\tfrac{r_n^2}{}\,\tfrac{\beta c_n(c_n^2-d_n^2)-\omega^2(1-\beta c_n)-(c_n^2+d_n^2)}{(r_n^2+M-\alpha\omega^2)^2+(2\alpha\omega c_n)^2}. \end{aligned} \tag{47}$$

On the basis of the last relations (43)–(46), it is easy to observe that the dimensionless steady state and transient components $w_{cs}(r,t)$, $w_{ct}(r,t)$ and $w_{ss}(r,t)$, $w_{st}(r,t)$ of $w_c(r,t)$ and $w_s(r,t)$, respectively, are given by the next relations

$$w_{cs}(r,t) = r\cos(\omega t)H(t) + 2\cos(\omega t)\sum_{n=1}^{\infty}\frac{J_1(rr_n)}{r_n J_0(r_n)}[H(t)-x_n] - 2\sin(\omega t)\sum_{n=1}^{\infty}\frac{y_n J_1(rr_n)}{r_n J_0(r_n)}, \tag{48}$$

$$w_{ct}(r,t) = 2\sum_{n=1}^{\infty}\frac{J_1(rr_n)}{r_n J_0(r_n)}[x_n\cosh(d_n t) + u_n\sinh(d_n t)]\,\mathrm{e}^{-c_n t}, \tag{49}$$

$$w_{ss}(r,t) = r\sin(\omega t) + 2\sin(\omega t)\sum_{n=1}^{\infty}\frac{J_1(rr_n)}{r_n J_0(r_n)}[H(t)-x_n] + 2\cos(\omega t)\sum_{n=1}^{\infty}\frac{y_n J_1(rr_n)}{r_n J_0(r_n)}, \tag{50}$$

$$w_{st}(r,t) = 2\sum_{n=1}^{\infty}\frac{J_1(rr_n)}{r_n J_0(r_n)}[-y_n\cosh(d_n t) + v_n\sinh(d_n t)]\,\mathrm{e}^{-c_n t}, \tag{51}$$

For the results' validation, it is necessary to use the fact that the steady-state components $w_{cs}(r,t)$ and $w_{ss}(r,t)$ of the starting velocity fields $w_c(r,t)$ and $w_s(r,t)$, respectively, can be presented in the equivalent forms

$$w_{cs}(r,t) = \mathrm{Re}\left\{\frac{I_1(r\sqrt{\delta})}{I_1(\sqrt{\delta})}\mathrm{e}^{i\omega t}\right\}, \quad w_{ss}(r,t) = \mathrm{Im}\left\{\frac{I_1(r\sqrt{\delta})}{I_1(\sqrt{\delta})}\mathrm{e}^{i\omega t}\right\}, \tag{52}$$

where $\delta = (i\omega\alpha + 1)(i\omega + M)/(i\omega\beta + 1)$. The simplified forms of the steady state velocities $w_{cs}(r,t)$ and $w_{ss}(r,t)$ from Equation (52) were obtained solving the corresponding steady boundary value problems. Figure 2 shows the equivalence of the expressions of $w_{cs}(r,t)$ and $w_{ss}(r,t)$ given by Equations (48) and (52) (left) and Equations (50) and (52) (right).

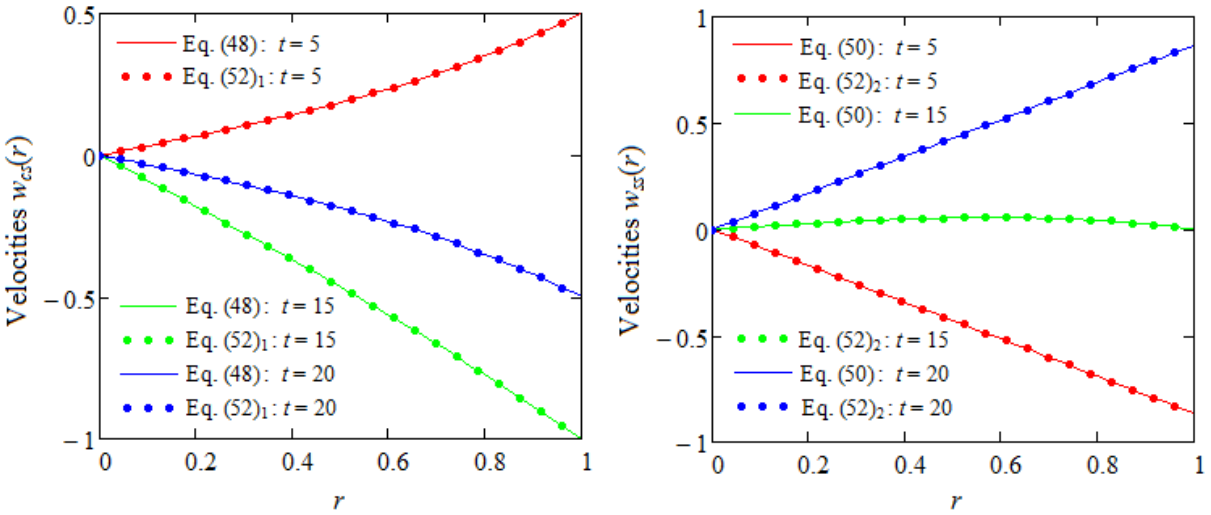

Figure 2. Equivalence of the expressions of $w_{cs}(r,t)$ and $w_{ss}(r,t)$ given by Equations (48) and (52) (left) and Equations (50) and (52) (right) for $\alpha = 0.6$, $\beta = 0.4$, $M = 0.8$ and $\omega = \pi/3$.

4.2. The Study Case When the Cylinder Rotates around Its Axis with the Velocity $VH(t)$

By taking $g(t) = VH(t)$ in Equation (43) and evaluating the convolution product or making $\omega = 0$ in Equation (44) (left), one finds the dimensionless starting velocity $w_C(r,t)$ corresponding to the MHD motion of ECIOBFs induced by the circular cylinder that rotates around its symmetry axis with the constant velocity V. It can also be presented as a sum of its steady and transient components, namely

$$w_C(r,t) = [w_{Cs}(r,t) + w_{Ct}(r,t)]H(t)\,, \tag{53}$$

in which $w_{Cs}(r)$ and $w_{Ct}(r,t)$ have the following expressions:

$$w_{Cs}(r) = r + 2M\sum_{n=1}^{\infty} \frac{J_1(rr_n)}{(r_n^2 + M)r_n J_0(r_n)}, \tag{54}$$

$$w_{Ct}(r,t) = 2\sum_{n=1}^{\infty} \frac{r_n J_1(rr_n)}{(r_n^2 + M)J_0(r_n)} \left[\cosh(d_n t) + \frac{c_n - \beta(c_n^2 - d_n^2)}{d_n}\sinh(d_n t)\right] \mathrm{e}^{-c_n t}. \tag{55}$$

An equivalent form for the dimensionless steady velocity $w_{Cs}(r)$, which is the same for Newtonian and non-Newtonian fluids, namely

$$w_{Cs}(r) = I_1(r\sqrt{M})/I_1(\sqrt{M}), \tag{56}$$

has been obtained making $\omega = 0$ in the Equality (52) (left). The equivalence of the expressions of $w_{Cs}(r)$ from Equalities (54) and (56) was also graphically proved.

As we already mentioned in the previous section, similar solutions for electrical conducting incompressible Maxwell fluids performing the same motions can be obtained by making $\beta = 0$ in the corresponding previous relations. The steady fluid velocity $w_{MCs}(r)$ corresponding to the last motion of Maxwell fluids is given by the relation (54) or (56), while the transient velocity $w_{MCt}(r,t)$ is given by the relation

$$w_{MCt}(r,t) = 2\sum_{n=1}^{\infty} \frac{r_n J_1(rr_n)}{(r_n^2+M)J_0(r_n)} \left[\cosh(b_n t) + \frac{a_n}{b_n}\sinh(b_n t)\right] \mathrm{e}^{-a_n t}, \tag{57}$$

where $a_n = (\alpha M+1)/2$ and $b_n = \sqrt{(\alpha M-1)^2 - 4\alpha r_n^2}/(2\alpha)$.

In all cases of the studied motions, in the absence of the magnetic field, the corresponding solutions can be immediately obtained by putting $M = 0$ in respective relations. By taking $M = 0$ in Equation (54) or making $M \to 0$ in Equation (56), one finds the dimensionless steady velocity $w_{Cs}(r) = r$ of the incompressible Oldroyd-B fluids induced by the circular cylinder that rotates around its axis with the constant velocity V.

5. Some Numerical Results and Conclusions

In the present study, two classes of MHD unsteady motions of ECIOBFs in an infinite circular cylinder that applies time-dependent longitudinal shear stress $Sf(t)$ to the fluid or rotates around its symmetry axis with the velocity $Vg(t)$ were analytically investigated. In the case of the first motion, general expressions have been established for the dimensionless non-trivial shear stress and the corresponding fluid velocity. For the results' validation, the expression of shear stress $\eta(r,t)$ was again obtained in Appendix A by using a different method. By making use of a simple observation regarding the governing equations of the shear stress in the case of the first motion and the fluid velocity in the second one, we directly obtained the dimensionless velocity field corresponding to the MHD unsteady motion of ECIOBFs induced by the circular cylinder that rotates around its symmetry axis with the velocity $Vg(t)$. In this way, two important classes of MHD unsteady motions of these fluids through an infinite circular cylinder were completely solved.

Later, for illustration and to bring to light some characteristics of the fluid behavior, some special cases were considered for the second class of motions of ECIOBFs, and the corresponding dimensionless starting velocity fields were provided. As the respective motions become steady in time, these velocity fields were presented as a sum of their steady and transient components. As a check of their correctness, the steady velocities were presented in two different forms whose equivalence was graphically proved in Figure 2. In practice, an important problem for experimental researchers is to know the need for time to reach a steady state. From a mathematical point of view, this is the time after which the diagrams of starting velocities overlap with those of their steady components. The influence of the magnetic field on this time and some characteristics of the fluid motion are graphically emphasized.

Figures 3–5 prove the convergence of dimensionless starting velocities $w_c(r,t)$, $w_s(r,t)$ and $w_C(r,t)$ given by Equations (44) (left), (44) (right) and (53), respectively, to their steady state or steady components $w_{cs}(r,t)$, $w_{ss}(r,t)$ and $w_{Cs}(r,t)$ for fixed values of the material constants, two distinct values of the magnetic parameter M and increasing values of the time t. From these figures, we can see the required time to touch the steady state for each motion that has been studied. The necessary time to obtain the steady state, as shown in Figures 3 and 4, is smaller for the motion due to sine oscillations of the cylinder than that corresponding to the motion induced by cosine oscillations of the cylinder. This is obvious because, at the moment $t = 0$, the velocity of the cylinder is zero. In all cases, the necessary time to obtain the steady state diminishes for increasing values of the parameter M. Consequently, the steady state in such motions of ECIOBFs is rather obtained in the presence of a magnetic field. A careful examination of Figure 5 indicates that the fluid velocity diminishes for increasing values of M. It means the fluid flows slower in the presence of a magnetic field.

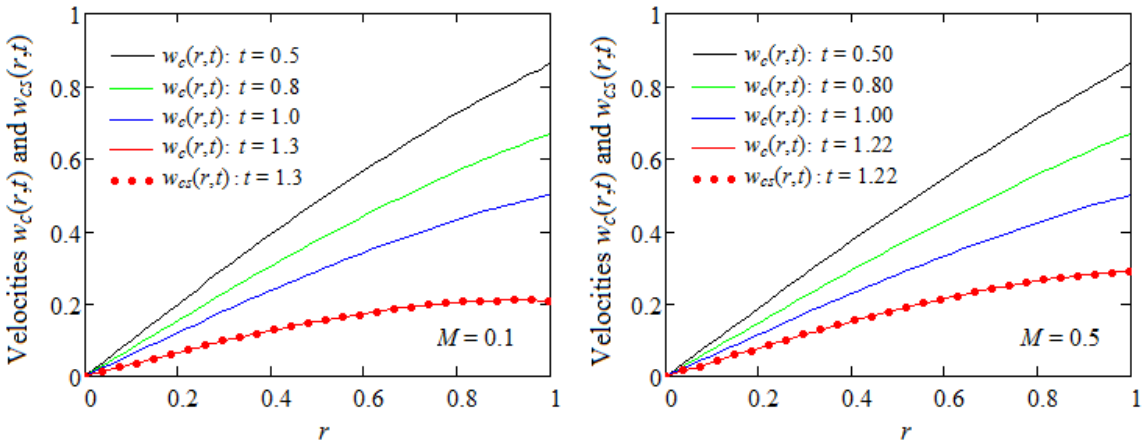

Figure 3. Convergence of the starting velocity $w_c(r,t)$ from Equation (44) (left) to its steady state component $w_{cs}(r,t)$ given by Equation (48) for $\alpha = 0.2$, $\beta = 0.1$, $\omega = \pi/3$, $M = 0.1$ or $M = 0.5$, and increasing values of t.

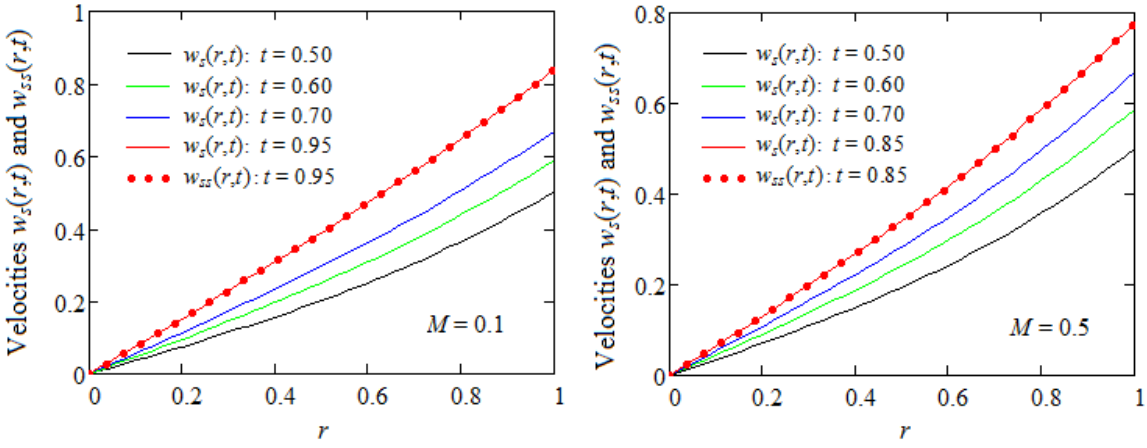

Figure 4. Convergence of the starting velocity $w_s(r,t)$ from Equation (44) (right) to its steady state component $w_{ss}(r,t)$ given by Equation (50) for $\alpha = 0.2$, $\beta = 0.1$, $\omega = \pi/3$, $M = 0.1$ or $M = 0.5$, and increasing values of t.

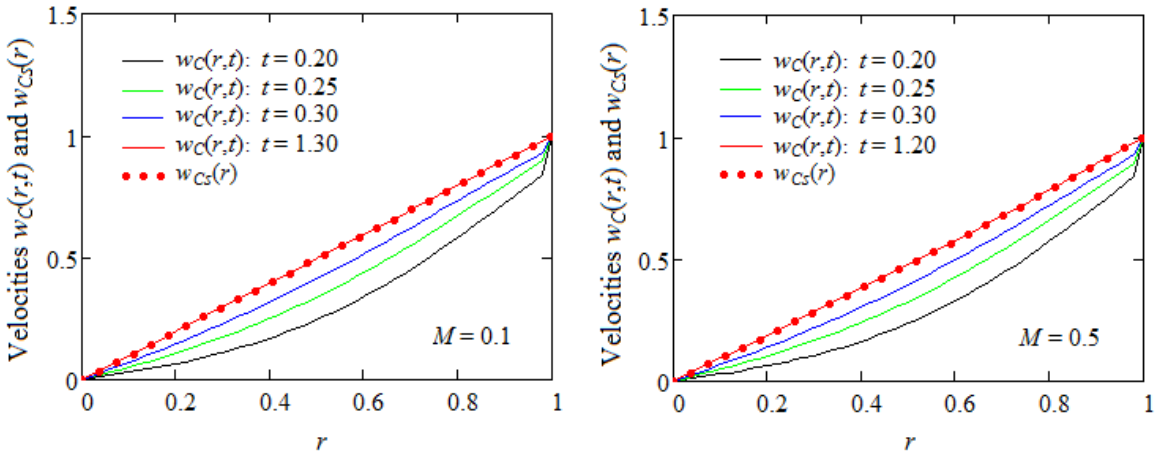

Figure 5. Convergence of the starting velocity $w_C(r,t)$ from Equation (53) to its steady component $w_{Cs}(r)$ given by Equation (54) for $\alpha = 0.2$, $\beta = 0.1$, $\omega = \pi/3$, $M = 0.1$ or $M = 0.5$, and increasing values of t.

Figures 6a–c and 7 present the behavior of the fluid in a motion in which the shear stress $\eta(r,t) = S_{rz}(r,t)$ is prescribed on the cylinder's surface and the function $f(t) = (e^{-t} - 1)/25$.

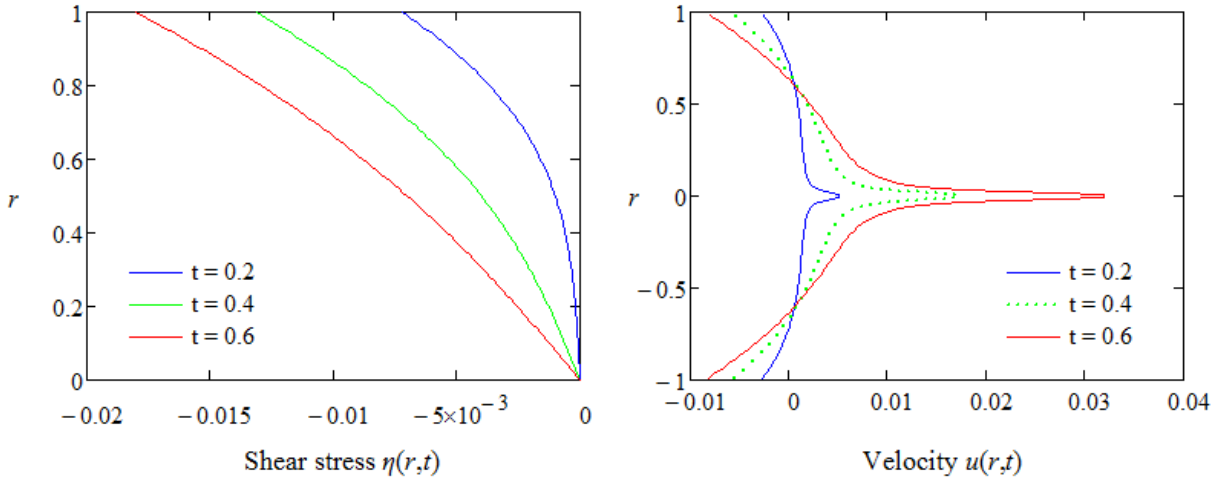

(**a**)

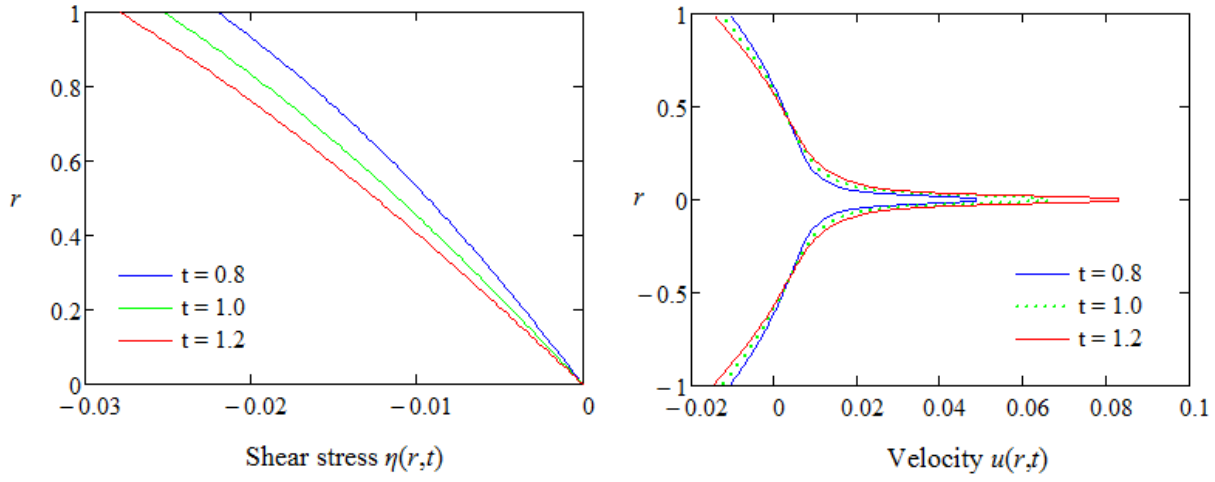

(**b**)

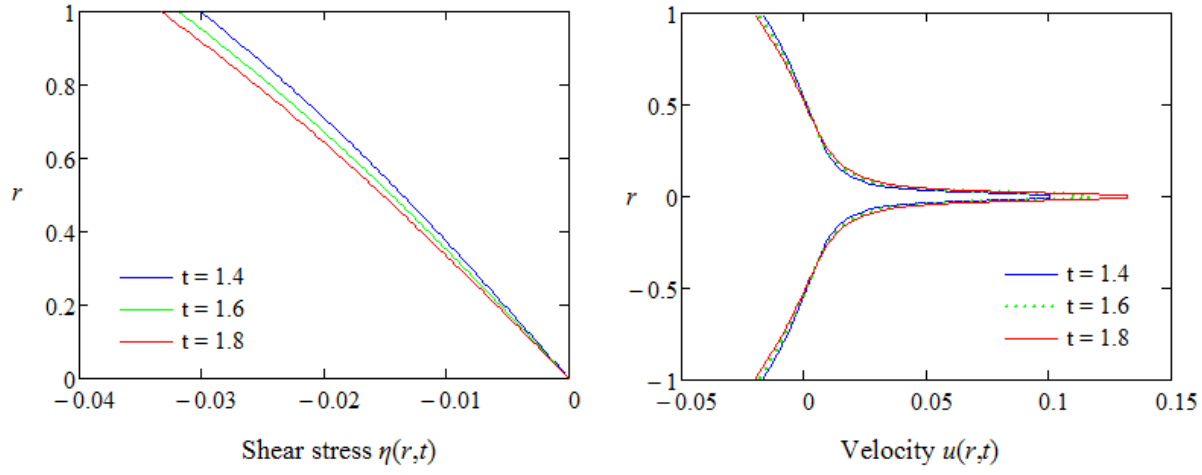

(**c**)

Figure 6. Profiles of shear stress $\eta(r,t)$ (**left**), and velocity $u(r,t)$ (**right**) given by the relations (23) and (32), respectively, for $\alpha = 0.5$, $\beta = 0.2$, $M = 0.8$ at different values of the time t. (**a**). Shear stress $\eta(r,t)$, and velocity $u(r,t)$ for $t \in \{0.2, 0.4, 0.6\}$. (**b**). Shear stress $\eta(r,t)$, and velocity $u(r,t)$ for $t \in \{0.8, 1.0, 1.2\}$. (**c**). Shear stress $\eta(r,t)$, and velocity $u(r,t)$ for $t \in \{1.4, 1.6, 1.8\}$.

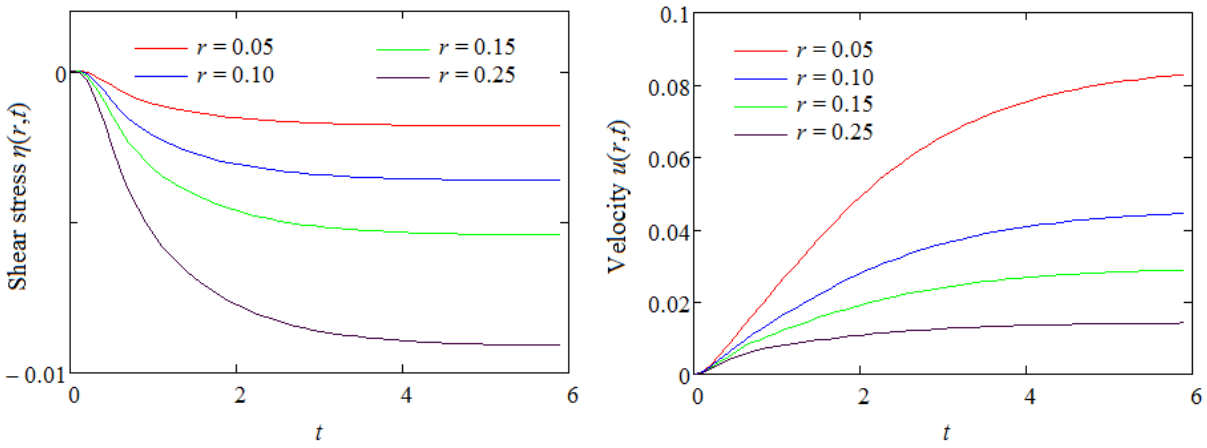

Figure 7. Profiles of shear stress $\eta(r,t)$ and velocity $u(r,t)$ are given by Relations (23) and (32), respectively, versus time for $\alpha = 0.5$, $\beta = 0.2$, $M = 0.8$ in different channel positions.

From these figures, one can see that the fluid layer located near the channel wall has reverse flow due to the shear stress that drives it in this movement. The central fluid layers flow in the opposite direction. The maximum velocity is achieved in the fluid layer located in the vicinity of the cylinder axis. This is achieved because the shear stress has a minimum value on the axis of the cylinder and increases with the distance from this axis. It should also be noted that with the increase in the time values, the velocities of the fluid layers become uniform. This property is due to the fact that the shear stress evens out its values over time.

The same properties are clearly highlighted in the graphs in Figure 7. In these graphs, it can be seen that for a certain time interval, the shear stress decreases, after which it tends to a constant value for each radial position of the channel. The fluid velocity has the same property. The shear stress property highlighted in Figure 7 can also be analytically justified if we use the following property of the Laplace transform $\lim_{t\to\infty} f(t) = \lim_{s\to 0} s\overline{f}(s)$. Indeed, using the Equalities (16) and (17), we obtain

$$\lim_{t\to\infty}\eta(r,t) = \lim_{s\to 0} s\overline{\eta}(r,s) = -2\lim_{s\to 0} s\overline{f}(s)\sum_{n=1}^{\infty}\frac{J_1(rr_n)}{J_0(r_n)}\frac{r_n}{r_n^2+a(s)}$$
$$-2\lim_{s\to 0} f(t)\sum_{n=1}^{\infty}\frac{J_1(rr_n)}{J_0(r_n)}\frac{r_n}{r_n^2+M}. \tag{58}$$

Equation (58) highlights that shear stress $\eta(r,t)$ tends to a constant value for large values of time t, if $\lim_{t\to\infty} f(t) < \infty$.

For the particular case analyzed in this section, $\lim_{t\to\infty} f(t) = \lim_{t\to\infty}\frac{e^{-t}-1}{25} = -\frac{1}{25}$, therefore

$$\lim_{t\to\infty}\eta(r,t) = \lim_{s\to 0} s\overline{\eta}(r,s) = \frac{2}{25}\sum_{n=1}^{\infty}\frac{J_1(r\,r_n)}{J_0(r_n)}\frac{r_n}{r_n^2+M}. \tag{59}$$

The main outcomes that have been obtained by this study are as follows:

- Closed-form expressions were established for dimensionless shear stress and velocity fields corresponding to MHD motions of ECIOBFs in an infinite circular cylinder that applies longitudinal shear stress $Sf(t)$ to the fluid.
- The dimensionless velocity of the MHD motion of the same fluids generated by the infinite circular cylinder that moves around its symmetry axis with the velocity $Vg(t)$ was directly obtained using one of the previous results.
- Consequently, the two types of MHD motions of ECIOBFs through an infinite circular cylinder were completely solved. For illustration, three particular cases were considered, and the corresponding velocity fields are provided.

- Graphical representations for starting and steady velocities of these unsteady motions, which become steady in time, showed that the steady state is obtained earlier and the fluid flows slower in the presence of a magnetic field.

Author Contributions: Conceptualization, C.F., D.V. and Z.I.; methodology, C.F. and D.V.; software, C.F., D.V. and Z.I.; validation, C.F., D.V. and Z.I.; formal analysis, C.F. and D.V.; investigation, C.F. and D.V.; resources, C.F. and D.V.; data curation, D.V.; writing—original draft preparation, C.F. and D.V.; writing—review and editing, C.F., D.V. and Z.I.; visualization, D.V.; supervision, C.F., D.V. and Z.I.; project administration, D.V. All authors have read and agreed to the published version of the manuscript.

Funding: This research received no external funding.

Data Availability Statement: Data are contained within the article.

Acknowledgments: The authors would like to express their sincere appreciation and thanks to the reviewers for their meticulous evaluation, valuable insights and constructive criticism.

Conflicts of Interest: The authors declare no conflicts of interest.

Appendix A

$$L^{-1}\left\{\frac{s+a}{(s+a)^2-b^2}\right\}=\mathrm{e}^{-at}\cosh(bt),\quad L^{-1}\left\{\frac{b}{(s+a)^2-b^2}\right\}=\mathrm{e}^{-at}\sinh(bt)\,. \tag{A1}$$

The first relation (13) can be also written as a modified Bessel equation

$$r^2\frac{\partial^2\overline{\eta}(r,s)}{\partial r^2}+r\frac{\partial\overline{\eta}(r,s)}{\partial r}-\left[1+\left[r\sqrt{a(s)}\right]^2\right]\overline{\eta}(r,s)=0, \tag{A2}$$

whose solution satisfying the corresponding boundary condition is

$$\overline{\eta}(r,s)=\overline{f}(s)\frac{I_1[r\sqrt{a(s)}]}{I_1[\sqrt{a(s)}]}=\overline{f}(s)\frac{J_1[ir\sqrt{a(s)}]}{J_1[i\sqrt{a(s)}]}=\overline{f}(s)\overline{H}(r,s). \tag{A3}$$

Applying the inverse Laplace transform to this last equality results in

$$\eta(r,t)=f(t)*H(r,t), \tag{A4}$$

where $H(r,t)$ is the inverse Laplace transform of $\overline{H}(r,s)$. In order to determine $H(r,t)$ by means of the residue theorem, the solutions of the transcendental equation $J_1[i\sqrt{a(s)}]=0$ are necessary. For each positive root r_n of the transcendental equation $J_1(r)=0$, it corresponds two roots of the equation $i\sqrt{a(s)}=r_n$, namely $s_{1n}=-c_n+d_n$ and $s_{2n}=-c_n-d_n$, which are defined in the Section 3.2.

It is a well-known fact that

$$H(r,t)=L^{-1}\{\overline{H}(r,s)\}=\sum_{n=1}^{\infty}\left\{\mathrm{e}^{s_{1n}t}\,Rez[\overline{H}(r,s)]\big|_{s=s_{1n}}+\mathrm{e}^{s_{2n}t}\,Rez[\overline{H}(r,s)]\big|_{s=s_{2n}}\right\}\,, \tag{A5}$$

in which the residues of $\overline{H}(r,s)$ in s_{1n} and s_{2n} are given by the relations:

$$Rez[\overline{H}(r,s)]\big|_{s=s_{1n}}=\left.\frac{J_1[ir\sqrt{a(s)}]}{\frac{d}{ds}\left\{J_1[i\sqrt{a(s)}]\right\}}\right|_{s=s_{1n}}=-2\frac{r_nJ_1(rr_n)}{J_0(r_n)}X_{1n}, \tag{A6}$$

$$Rez[\overline{H}(r,s)]\big|_{s=s_{2n}} = \left.\frac{J_1[ir\sqrt{a(s)}]}{\frac{d}{ds}\left\{J_1[i\sqrt{a(s)}]\right\}}\right|_{s=s_{2n}} = -2\frac{r_n J_1(rr_n)}{J_0(r_n)}X_{2n}. \tag{A7}$$

In the last two relations, X_{1n} and X_{2n} have the expressions

$$X_{1n} = \frac{\beta^2 s_{1n}^2 + 2\beta s_{1n} + 1}{\alpha\beta s_{1n}^2 + 2\alpha s_{1n} + (\alpha-\beta)M + 1} \quad \text{and} \quad X_{2n} = \frac{\beta s_{2n}^2 + 2\beta s_{2n} + 1}{\alpha\beta s_{2n}^2 + 2\alpha s_{2n} + (\alpha-\beta)M + 1}. \tag{A8}$$

From Equations (A5)–(A7), it results that

$$\begin{aligned} H(r,t) &= -2\sum_{n=1}^{\infty}\frac{r_n J_1(rr_n)}{J_0(r_n)}\left(X_{1n}e^{d_n t} + X_{2n}e^{-d_n t}\right)\, e^{-c_n t} \\ &= -2\sum_{n=1}^{\infty}\frac{r_n J_1(rr_n)}{J_0(r_n)}[(X_{1n}+X_{2n})\cosh(d_n t) + (X_{1n}-X_{2n})\sinh(d_n t)]\, e^{-c_n t}. \end{aligned} \tag{A9}$$

Lengthy but straightforward computations show that

$$X_{1n} + X_{2n} = \frac{\beta}{\alpha}, \quad X_{1n} - X_{2n} = \frac{1-\beta c_n}{\alpha d_n}. \tag{A10}$$

Now, by substituting $X_{1n} + X_{2n}$ and $X_{1n} - X_{2n}$ from (A10) in (A9), one finds that

$$H(r,t) = -\frac{2}{\alpha}\sum_{n=1}^{\infty}\frac{r_n J_1(rr_n)}{J_0(r_n)}\left[\beta\cosh(d_n t) + \frac{1-\beta c_n}{d_n}\sinh(d_n t)\right] e^{-c_n t}, \tag{A11}$$

or equivalently

$$H(r,t) = r\delta(t) + 2\sum_{n=1}^{\infty}\frac{J_1(rr_n)}{r_n J_0(r_n)}\left\{\delta(t) - \frac{r_n^2}{\alpha}\left[\beta\cosh(d_n t) + \frac{1-\beta c_n}{d_n}\sinh(d_n t)\right]e^{-c_n t}\right\}. \tag{A12}$$

Finally, by substituting the function $H(r,t)$ from Equation (A12) in (A4), one recovers the same expression (23) for the dimensionless shear stress $\eta(r,t)$.

References

1. Oldroyd, J.G. On the formulation of rheological equations of state. *Proc. R. Soc. London Ser. A* **1950**, *200*, 523–541. [CrossRef]
2. Waters, N.D.; King, M.J. The unsteady flow of an elastico-viscous liquid in a straight pipe of circular cross section. *J. Phys. D Appl. Phys.* **1971**, *4*, 204–211. [CrossRef]
3. Rajagopal, K.R.; Bhatnagar, R.K. Exact solutions for simple flows of an Oldroyd-B fluid. *Acta Mech.* **1995**, *113*, 233–239. [CrossRef]
4. Wood, W.P. Transient viscoelastic helical flow in pipes of circular and annular cross-section. *J. Non-Newton. Fluid Mech.* **2001**, *100*, 115–126. [CrossRef]
5. Fetecau, C. Analytical solutions for non-Newtonian fluid flows in pipe-like domains. *Int. J. Non-Linear Mech.* **2004**, *39*, 225–231. [CrossRef]
6. Fetecau, C.; Fetecau, C.; Vieru, D. On some helical flows of Oldroyd-B fluids. *Acta Mech.* **2007**, *189*, 53–63. [CrossRef]
7. McGinty, S.; McKee, S.; McDermott, R. Analytic solutions of Newtonian and non-Newtonian pipe flows subject to a general time-dependent pressure gradient. *J. Non-Newton. Fluid Mech.* **2009**, *162*, 54–77. [CrossRef]
8. Fetecau, C.; Imran, M.; Fetecau, C. Taylor-Couette flow of an Oldroyd-B fluid in an annulus due to a time-dependent couple. *Z. Naturforsch.* **2011**, *66*, 40–46. [CrossRef]
9. Jamil, M.; Khan, N.A. Axial Couette flow of an Oldroyd-B fluid in an annulus. *Theor. Appl. Mech. Lett.* **2012**, *2*, 012001. [CrossRef]
10. Imran, M.; Tahir, M.; Imran, M.A.; Awan, A.U. Taylor-Couette flow of an Oldroyd-B fluid in an annulus subject to a time dependent rotation. *Am. J. Appl. Math.* **2015**, *3*, 25–31. [CrossRef]
11. Ullah, S.; Tanveer, M.; Bajwa, S. Study of velocity and shear stress for unsteady flow of incompressible Oldroyd-B fluid between two concentric rotating circular cylinders. *Hacet. J. Math. Stat.* **2019**, *48*, 372–383. [CrossRef]
12. Baranovskii, E.S.; Artemov, M.A. Optimal Dirichlet boundary control for the corotational Oldroyd model. *Mathematics* **2023**, *11*, 2719. [CrossRef]
13. Khan, M.; Malik, R.; Anjun, A. Analytic solutions for MHD flows of an Oldroyd-B fluid between two side walls perpendicular to the plate. *Chem. Eng. Commun.* **2011**, *198*, 1415–1434. [CrossRef]
14. Zahid, M.; Rana, M.A.; Haroon, T.; Siddiqui, A.M. Applications of Sumudu transform to MHD flows of an Oldroyd-B fluid. *Appl. Math. Sci.* **2013**, *7*, 7027–7036. [CrossRef]

15. Ghosh, A.K.; Datta, S.K.; Sen, P. On hydromagnetic flow of an Oldroyd-B fluid between two oscillating plates. *Int. J. Appl. Comput. Math.* **2016**, *2*, 365–386. [CrossRef]
16. Tan, W.C.; Masuoka, T. Stokes' first problem for an Oldroyd-B fluid in a porous medium. *Phys. Fluids* **2005**, *17*, 023101. [CrossRef]
17. Khan, I.; Imran, M.; Fakhar, K. New exact solutions for an Oldroyd-B fluid in a porous medium. *Int. J. Math. Math. Sci.* **2011**, *2011*, 408132. [CrossRef]
18. Hayat, T.; Shehzad, S.A.; Mustafa, M.; Hendi, A. MHD flow of an Oldroyd-B fluid through a porous channel. *Int. J. Chem. React. Eng.* **2012**, *10*. [CrossRef]
19. Sultan, Q.; Nazar, M.; Ali, U.; Imran, M. Unsteady flow of Oldroyd-B fluid through porous rectangular duct. *Int. J. Nonlinear Sci.* **2013**, *15*, 195–211.
20. Khan, I.; Ijaz, A. Starting solutions for an MHD Oldroyd-B fluid through porous space. *J. Porous Media* **2014**, *17*, 797–809. [CrossRef]
21. Hayat, T.; Hussain, M.; Khan, M. Hall effect on flows of an Oldroyd-B fluid through porous medium for cylindrical geometries. *Comput. Math. Appl.* **2006**, *52*, 269–282. [CrossRef]
22. Hamza, S.E.E. MHD flow of an Oldroyd-B fluid through porous medium in a circular channel under the effect of time dependent pressure gradient. *Am. J. Fluid Dyn.* **2017**, *7*, 1–11. [CrossRef]
23. Riaz, M.B.; Awrejcewicz, J.; Rehman, A.U. Functional effects of permeability on Oldroyd-B fluid under magnetization: A comparison of slipping and non-slipping solutions. *Appl. Sci.* **2021**, *11*, 11477. [CrossRef]
24. Fetecau, C.; Vieru, D. Investigating magnetohydrodynamic motions of Oldroyd-B fluids through a circular cylinder filled with porous medium. *Processes* **2024**, *12*, 1354. [CrossRef]
25. Fetecau, C.; Vieru, D. Memory effects in the magnetohydrodynamic axial symmetric flows of Oldroyd-B fluids in a porous channel. *Symmetry* **2024**, *16*, 1108. [CrossRef]
26. Fetecau, C.; Rauf, A.; Qureshi, T.M.; Vieru, D. Steady-state solutions for MHD motions of Burgers fluids through porous media with differential expressions of shear on the boundary and applications. *Mathematics* **2022**, *10*, 4228. [CrossRef]
27. Sneddon, I.N. *Fourier Transforms*; McGraw-Hill Book Company, Inc.: New York, NY, USA, 1951.